Aquaculture 611 (2026) 743007

Contents lists available at ScienceDirect

Aquaculture

journal homepage: www.elsevier.com/locate/aquaculture

Disrupted gonadal development and associated alterations in meat yield and physiological response in triploid Pacific abalone, *Haliotis discus hannai*

Yi Wang [a,b], Jianpeng Zhang [a,b], Yang Gan [c], Yexin Chen [c], Weiwei You [a,b,d], Xuan Luo [a,b,c,*], Caihuan Ke [a,b,d,*]

[a] State Key Laboratory of Mariculture Breeding, College of Ocean and Earth Sciences, Xiamen University, Xiamen 361102, China
[b] Fujian Key Laboratory of Genetics and Breeding of Marine Organisms, College of Ocean and Earth Sciences, Xiamen University, Xiamen 361102, China
[c] Abalone Research Center, Fujian Minruibao Marine Biotechnology Co., Ltd, Xiamen 361102, China
[d] Fujian Ocean Innovation Center, Xiamen 361102, China

ARTICLE INFO

Keywords:
Gametogenesis
Gonad bulk index
Haliotis discus hannai
Meat yield
Steroid hormones
Triploid

ABSTRACT

The extent of reduced fecundity in triploid shellfish exhibits significant variation and is primarily correlated with the alteration of physiological and metabolic responses. In this study, the reproductive performance of diploid and triploid *Haliotis discus hannai* was analyzed throughout the reproductive cycle, focusing on gonadal development, steroid hormone levels, and corresponding changes in the foot muscle-soft tissue index (FMSI). A targeted division criterion for assessing gonadal development in triploid abalone was established. The results demonstrated that the ability to produce functional gametes was maintained in triploid females, while in triploid males, spermatogenesis was interrupted at the spermatocyte stage. More specifically, triploid ovarian development was characterized by the appearance of massive oogonia in the follicles, whereas apoptotic or autophagic cells were observed in the developing triploid testis. The estradiol and testosterone levels in triploid gonads dropped significantly at the stagnant stages; hence, insufficient steroid levels may be related to reproductive impairment. Additionally, there was a significant decrease in gonadal fullness in triploids during the maturation season, as indicated by the gonad bulk index (GBIn). The relationships between GBIn and FMSI, as well as their impact on gender, further suggest that gonadal development negatively affects FMSI, particularly since female triploids exhibit decreased gonadal fullness and increased FMSI. These findings have clarified the disruption of gonadal development and associated alterations in meat yield and physiological responses in triploid *H. discus hannai*, and thus are relevant to the development of breeding strategies for triploid abalone.

1. Introduction

Chromosome manipulation, the most common approach to genetic improvement, has been achieved in many species of fish and shellfish, resulting in the production of populations and lineages of ploidy-controlled, sterile, or monosex individuals (Das, 2014). The resulting triploids typically exhibit reduced fertility. This impairment of gonadal development is highly variable (sex and species-specific) in most triploid aquatic animals and has been roughly categorized into four patterns: (1) complete sterility in both females and males; in some species, such as gilthead sea bream *Sparus aurata* (Haffray et al., 2005) and blacklip abalone *Haliotis rubra* (Liu et al., 2009), triploids have incomplete gonadal development and do not form mature gametes. (2) female fertility and male sterility: some induced triploids are only able to produce relatively small numbers of oocytes but not spermatozoa, such as in the turbot *Scophthalmus maximus* (Cal et al., 2006) and the Pacific oyster *Crassostrea gigas* (chemical triploid) (Normand et al., 2008). (3) female sterility and male fertility: certain triploids lack mature oocytes in the ovaries but contain a small number of differentiated spermatozoa in the testis, for example, grass carp *Ctenopharyngodon idella* (Zajicek et al., 2011) and Atlantic salmon *Salmo salar* (Murray et al., 2018). (4) partial sterility in both sexes: species such as gibel carp *Carassius gibelio* (Przybyl et al., 2022) and *C. gigas* (mated triploid) (Qin et al., 2022) retained the ability to produce partially viable gametes. There are stark alterations in gametogenesis and gonadal development in triploid aquatic animals, and the vast majority of gonadal characteristics in triploids have been

* Corresponding authors at: Fujian Key Laboratory of Genetics and Breeding of Marine Organisms, College of Ocean and Earth Sciences, Xiamen University, Xiamen 361102, China.
E-mail addresses: xluo@xmu.edu.cn (X. Luo), chke@xmu.edu.cn (C. Ke).

https://doi.org/10.1016/j.aquaculture.2025.743007
Received 21 March 2025; Received in revised form 26 July 2025; Accepted 26 July 2025
Available online 28 July 2025

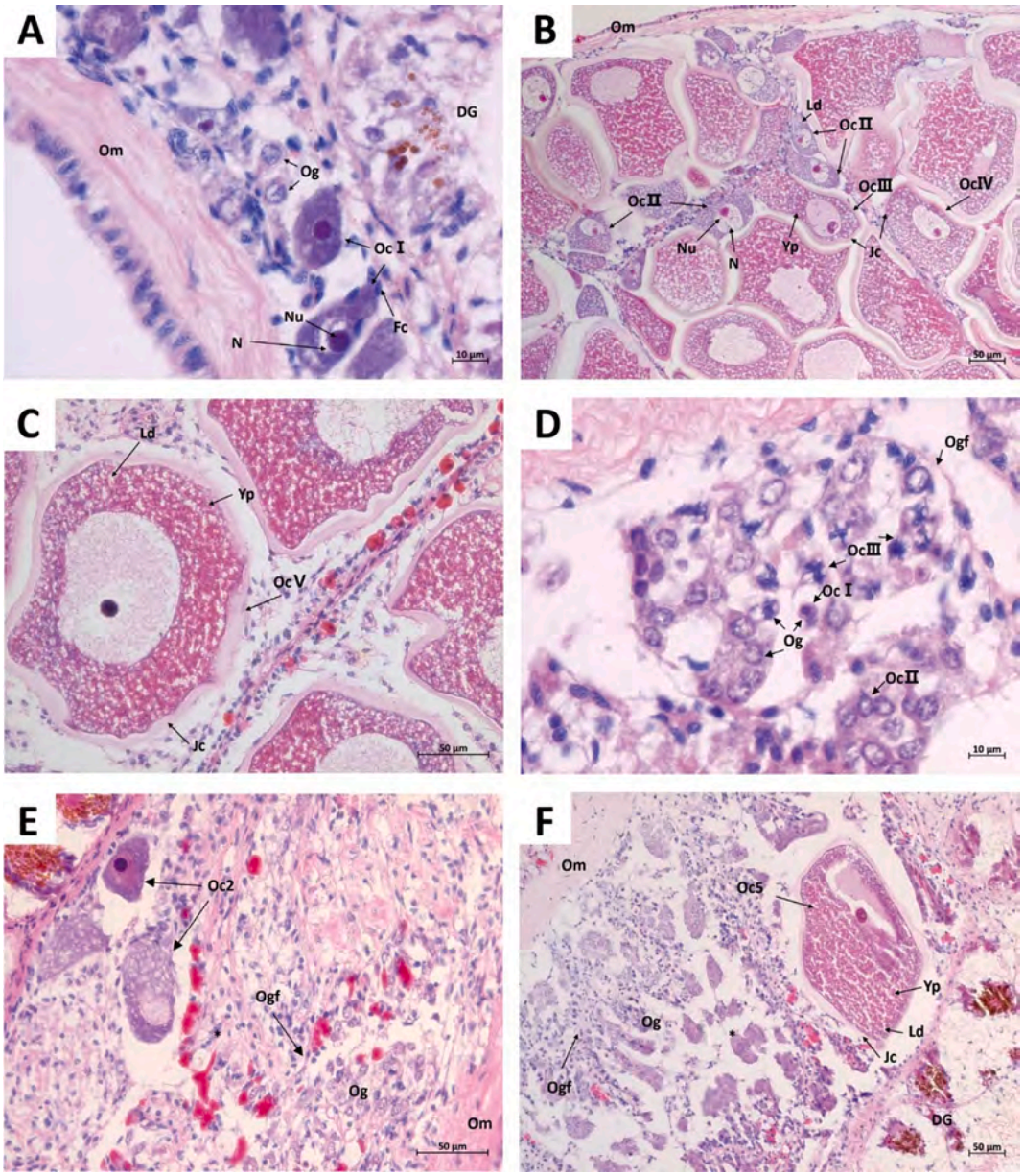

Fig. 1. Types of germ cells of oogenesis at the light microscopic level in diploid (DD 2 N) and triploid (DD 3 N) *H. discus hannai*. A–C: diploid ovary, D–F: triploid ovary. Og: oogonia, Oc1: stage I oocyte, Oc2: stage II oocyte, Oc3: stage III oocyte, Oc4: stage IV oocyte, Oc5: stage V oocyte, Og I: type I oogonia, Og II: type II oogonia, Og III: type III oogonia, Fc: follicular cell, N: nucleus, Nu: nucleolus, Ld: lipid droplet, Yp: yolk granule, Es: egg stalk, Jc: jelly coat, Ogf: oogenic follicle, Om: ovarian outer membrane, DG, digestive gland.

assessed by referencing diploids. Among the existing research, classification systems specific to triploid development have been established only for the eastern oyster *Crassostrea virginica* (Matt and Allen, 2021) and for *C. gigas* (Jouaux et al., 2010; Yang et al., 2022b).

The inhibition of gonad development also means that individuals likely demonstrate enhancements in other metabolic activities, such as growth, adaptability, and nutritional quality (Piferrer et al., 2009; Brianik and Allam, 2023). Rapid growth and/or increased biomass have been observed in most triploid species, and this advantage is most likely attributed to the redistribution of energy from gonadogenesis to other metabolic processes. For example, the triploids of *S. maximus* showed increased biomass and size homogeneity, and this economic advantage was attributed to the higher proportion of rapidly growing females (with smaller and rudimentary gonads) within the population (Cal et al., 2006). In Nile tilapia *Oreochromis niloticus* (Carman et al., 2023) and blue mussel *Mytilus edulis* (Osterheld et al., 2024), triploids exhibited poorly developed gonads and a reduced gonadosomatic index, indicating that less energy was devoted to reproduction. The induced triploid marine medaka *Oryzias dancena* reportedly showed better growth, accompanied by decreases in the gonadosomatic index as well as the concentrations of testosterone (T) and estradiol-17β (E2) (Park et al., 2016). Triploid salmonids also exhibited low levels of reproductive neuropeptides, sex steroids, and vitellogenin during the reproductive cycle (Tiwary et al., 2002; Piferrer et al., 2009). However, the research on gonadal development in triploid shellfish has generally focused on microstructural observations of gonadal development and gametogenesis, with limited studies examining the alterations in growth or other physiological processes associated with gonadal development.

Abalone, with their adductor muscle as the primary edible part, have considerable commercial value among consumers in the international market (Gao et al., 2022). As the leading global producer, China's annual cultured abalone output reached 244,991 tons in 2023, with the

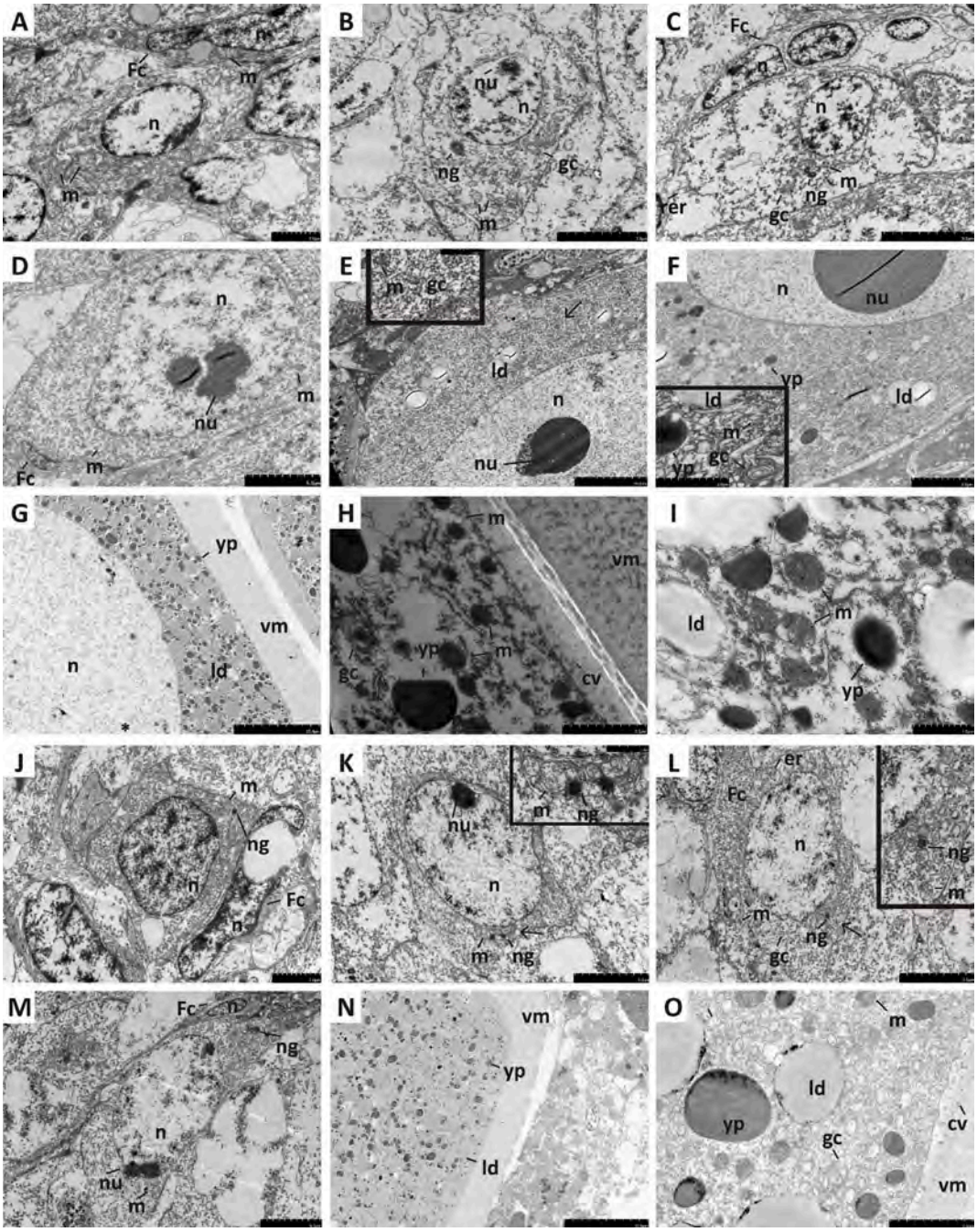

Fig. 2. Transmission electron micrographs of oogenesis in diploid (DD 2 N) and triploid (DD 3 N) *H. discus hannai*. A range of female germ cells derived from diploids were observed, as oogonia (A–C), stage I oocyte (D), stage II oocyte (E), stage III oocyte (F), and stage IV–V oocyte (G–I). The oogonia (J–L), stage I oocyte (M), and stage V oocyte (N–O) of the female triploid were synchronous observed. Inset: enlarged view at the black arrow, Fc: follicular cell, n: nucleus, nu: nucleolus, ng: nuage, m: mitochondria, gc: Golgi complex, ld: lipid droplet, yp: yolk granule, vm: vitelline envelope, cv: coated vesicles.

Pacific abalone, *Haliotis discus hannai*, being the dominant farmed species (China Bureau of Fisheries, 2024; FAO, 2024). Nevertheless, abalone generally grow at a rate of 2–3 cm per year and attain an approximate market size within 2–3 years (Arai and Okumura, 2013). This feature of slow growth is regarded as a significant constraint to the productivity of abalone aquaculture. As a result, numerous studies on triploid abalone have been published based on triploid induction. Some studies have concluded that triploid abalones have definite advantages in growth and meat yield due to their sterility and heterozygosity (Arai and Okumura, 2013; Wang et al., 2022). Reports on the gonadal development of triploid *H. discus hannai* are generally inconsistent regarding the degree of gametogenesis, and other physiological processes associated with gonadal development, such as hormonal regulation as well as the trade-off between growth and reproduction, have yet to be fully evaluated (Li et al., 2004; Yan et al., 2005; Jee et al., 2013; Kim et al., 2019).

Therefore, the histology and cytology of gonadal development, as well as the concentrations of sex steroids in the gonads of triploid and diploid *H. discus hannai*, were evaluated throughout a complete reproductive cycle. The foot muscle-soft tissue index (FMSI) and gonad bulk index (GBIn) were measured to examine the differences in resource allocation between reproduction and growth. The objective of this study was to provide insight into the alterations in gonad development and associated physiological metabolic processes of triploid *H. discus hannai*.

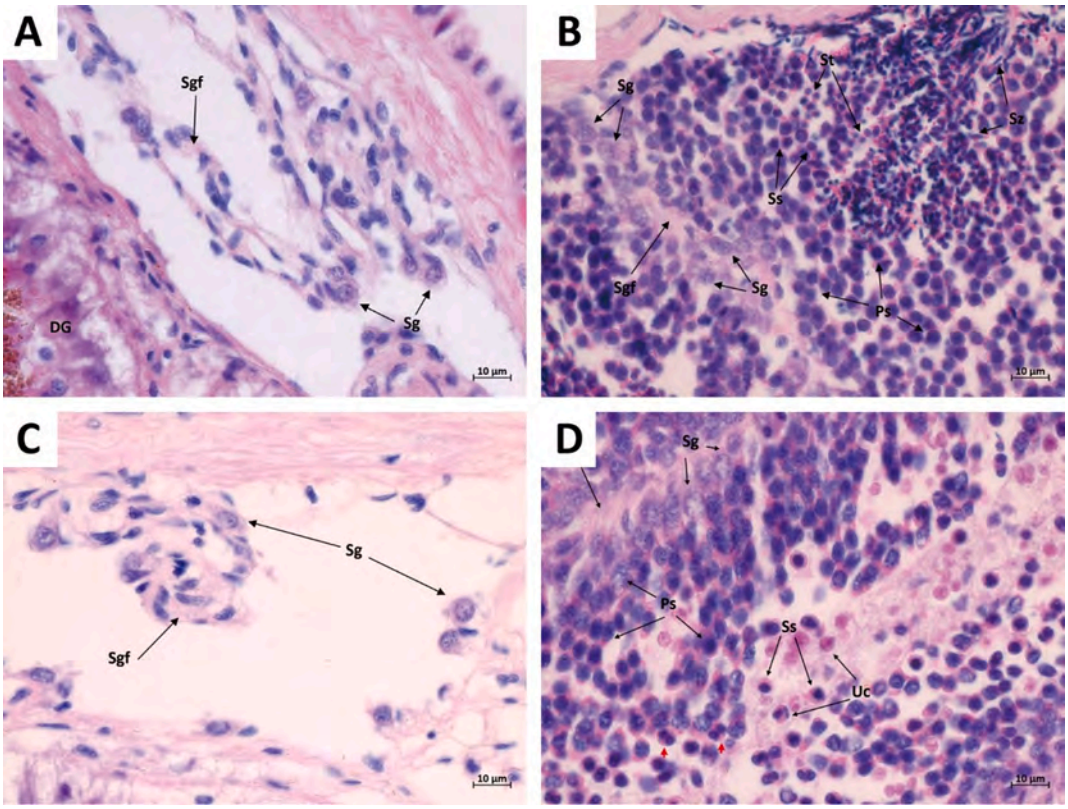

Fig. 3. Types of germ cells of spermatogenesis at the light microscopic level in diploid (DD 2 N) and triploid (DD 3 N) *H. discus hannai*. A–B: diploid testis (1000×), C–D: triploid testis (1000×). Sg: spermatogonia, Ps: primary spermatocytes, Ss: secondary spermatocytes, St: spermatids, Sz: spermatozoa, Uc: dividing spermatocytes, red arrow: vacuole-like cells, Sgf: spermatogenesis follicle. (For interpretation of the references to colour in this figure legend, the reader is referred to the web version of this article.)

2. Materials and methods

2.1. Abalone sampling and morphometry

Triploid and diploid abalone in this study were derived from the same batch of individuals as those described in Wang et al. (2022). Triploid and sibling diploid *H. discus hannai* were descendants from the same multiple parents (15 females and 5 males), in which the triploids were produced by inhibiting meiosis II using 30 mg L^{-1} of 6-dimethylaminopurine (6-DMAP). The abalone were raised in sea-based suspended systems (23°46′ N, 117°32′ E) in Zhangzhou, Fujian Province, at seven months post-fertilization (mpf). The initial shell lengths and rearing conditions (cultivation density and feeding) of the diploids and triploids were consistent in the sea-based aquaculture mode. From 20 mpf to 28 mpf, 30 diploids and 30 triploids adult abalones from 3 to 5 baskets (6–10 individuals/basket) were randomly sampled every two months for measuring body size (body weight, shell weight, and foot muscle weight) and calculating the foot muscle soft tissue index (FMSI = foot muscle weight/the difference between body weight and shell weight). The hemolymph and gonads of the abalone were then immediately dissected for ploidy determination and assessment of gonad development. The dissected gonad from each individual was divided into three parts; the tip of conical organ was placed in 4 % paraformaldehyde (PFA) and fixed overnight (4 °C) for histological observations, and a small piece of gonad (1 cm^3) was fixed for 24 h (4 °C) using 2.5 % glutaraldehyde in 0.1 M phosphate buffer solution (pH 7.4) for transmission electron microscope (TEM) observations. The remaining gonad tissue was frozen in liquid nitrogen and stored at −80 °C for steroid analysis. The water temperature range at the time of sampling for the sea-based suspension system was 13.98 °C to 28.24 °C.

2.2. Ploidy determination

Ploidy levels were detected using flow cytometry (CytoFLEX, Beckman Coulter, USA) and DAPI DNA staining as described by Wang et al. (2022). In brief, 200 μL of hemolymph was extracted from each individual, and the precipitated cell pellet was mixed with 0.5 mL of DAPI/detergent/DMSO solution for nuclear staining. Ploidy levels of each individual were calculated with reference to the DNA content of diploids using ModFit LT (version 5.0.9). Triploid individuals identified in the induced population were selected for subsequent analysis.

2.3. Histological analysis

Following dissection, the fixed conical tips of the gonads were embedded in paraffin wax and sectioned at 5 μm thickness. The deparaffinized sections were stained with hematoxylin-eosin (HE) and observed under a microscope (Olympus Axio Imager A2, Olympus Corporation, Tokyo, Japan). The cell types of the gametes in diploid and triploid abalone were identified using the histological characteristics of germ cells in the tropical abalone *Haliotis asinina* and the triploid *C. virginica* as described by Apisawetakan et al. (1997), Roux et al. (2013), and Matt and Allen (2021). The distinct stages of reproductive development in diploid *H. discus hannai* were classified according to previous morphological criteria, where the stages were distinguished primarily based on the cell types within the follicles. Considering the abnormal gonad development of triploid abalones, the classification of the gonadal development stage was assigned based on multiple features, including the extent of follicle development, the type and relative abundance of cells in the follicles, and the proportion of connective tissue in the follicles. The abalone were assigned into three groups for sex ratio determination: (1) females, identified by the presence of

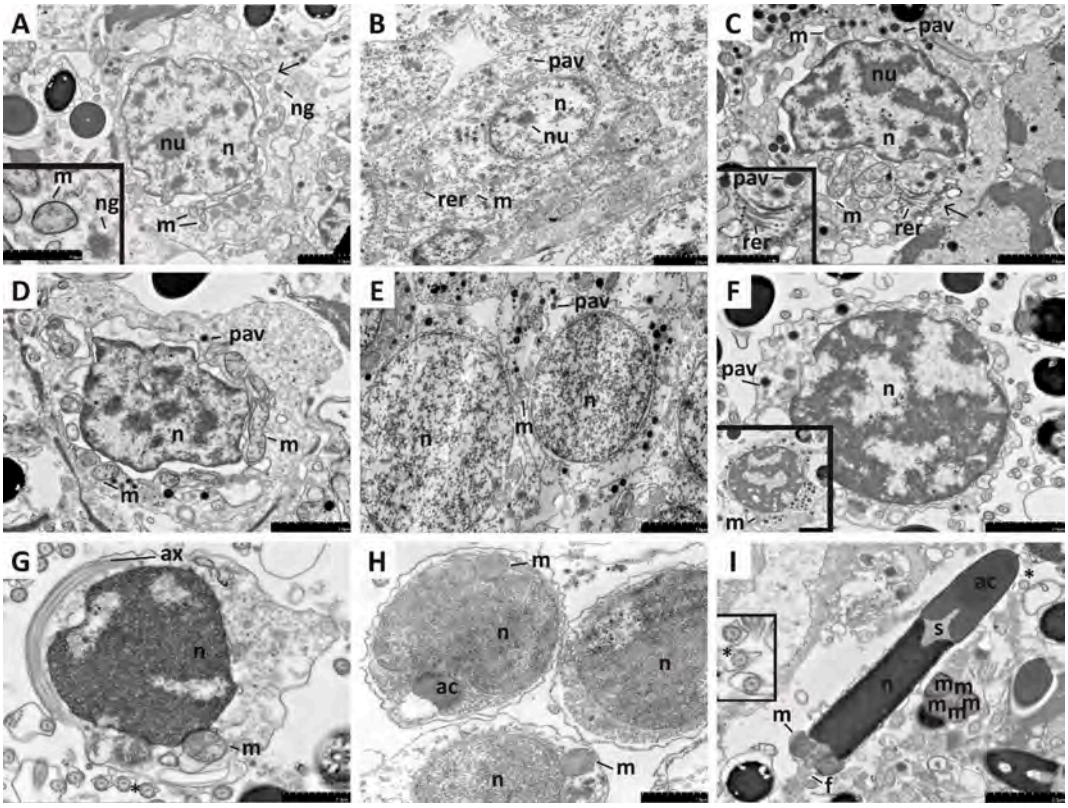

Fig. 4. Transmission electron micrographs of spermiogenesis in diploid *H. discus hannai*. A: spermatogonia, B: early primary spermatocytes, C–D: medium-term primary spermatocytes, E: late primary spermatocytes, F: secondary spermatocytes, G: early spermatids, H: late spermatids, I: spermatozoa. Inset: enlarged view at the black arrow, n: nucleus, nu: nucleolus, ng: nuage, m: mitochondria, pav: proacrosomal vesicle, rer: rough endoplazmik reticulum, ax: axoneme, ac: acrosome, s: subacrosomal space, *: flagellum with the 9 + 2 arrangement of microtubules.

oogenetic cells in the follicles, (2) males, determined by the presence of spermatogenic cells in the follicles, and (3) inactive, lacking oogenetic and spermatogenic cells.

The gonad bulk index (GBIn) of each individual was calculated by the method of Newman (1967) to evaluate the fullness of the gonads in diploid and triploid abalone. The global view of the cross-section of the conical appendages (two or three views per individual) was scanned at low magnification using a stereomicroscope (M165C, Leica Microsystems, Singapore). The cross-sectional area (total area of the section) of conical tissue and the area of the hepatopancreas were measured using LAS (version 4.13.0) software (Leica Microsystems), and the gonadal area was subsequently calculated as the difference of the two areas. The GBIn for assessing the relative proportion of gonads from the conical appendage was calculated according to the following equation:

$$GBIn = \frac{Gonadal\ area}{Total\ area\ of\ section} \times 100$$

Subsequently, gonadal sections were collected from diploid and triploid females during the breeding season (October). The gonadal area of the conical appendages was measured, and the number of mature oocytes within that area was quantified. The mature oocyte count per unit area was then used to estimate the effective number of viable gametes in females, as detailed in the calculation below:

$$Mature\ oocyte\ count\ per\ unit\ area = \frac{Mature\ oocyte\ count}{Gonadal\ area} \times 100$$

2.4. Cytological analysis

After determining the histological characteristics of gonad development in each individual, gonad tissues demonstrating the designated gametogenic features (encompassing all germ cell types) were selected for ultrastructural observation. Corresponding fixed samples were rinsed three times with 0.1 M phosphate buffer (pH 7.4) and then transported to the core facility of biomedical sciences (Xiamen University) for further embedding and slicing. Ultrathin sections (70 nm) were mounted on copper grids and stained with uranyl acetate and lead citrate. Images were obtained using a TEM (HT-7800, Hitachi, Japan). The cytological characteristics of gametogenesis in the samples were identified according to those used for *H. asinina* (Sobhon et al., 2001), the abalones *Haliotis ovina* (Singhakaew et al., 2003) and *Haliotis varia* (Najmudeen, 2008), the Manila clam *Ruditapes philippinarum* (Lee, 2008), the razor clam *Sinonovacula constricta* (Chung et al., 2008), and *C. gigas* (Franco et al., 2008).

2.5. Sex steroid analysis

Gonadal tissues from each development stage were freeze-dried (Labconco FreeZone 4.5 Plus, Kansas City, MO, USA) overnight at −70 °C. Several samples (2–6 individuals) derived from single or mixed stages were pooled to form one biological replicate, resulting in three biological replicates per period for steroid analysis. Steroid extraction was conducted according to a modified Arbor Assays® tissue extraction protocol. In brief, 30–60 mg of freeze-dried sample was homogenized in acetonitrile (1.5 mL) using a cryogenic tissue grinder (Q24, DHS, Beijing, China) at 4 °C. The tissue homogenate was centrifuged at 10,000 ×*g* and 4 °C for 10 min. The supernatant was transferred to a clean tube containing 3 mL of hexane, and the mixture was vortexed for 5 min. The acetonitrile phase (at the bottom) was transferred into a clean tube and evaporated to dryness using a Speedvac (EZ-2, Genevac, UK). The resulting residue was then stored at −20 °C.

The concentrations of E2 and T in the gonad were measured using an Arbor Assays® DetectX 17β-Estradiol ELISA kit and a Testosterone

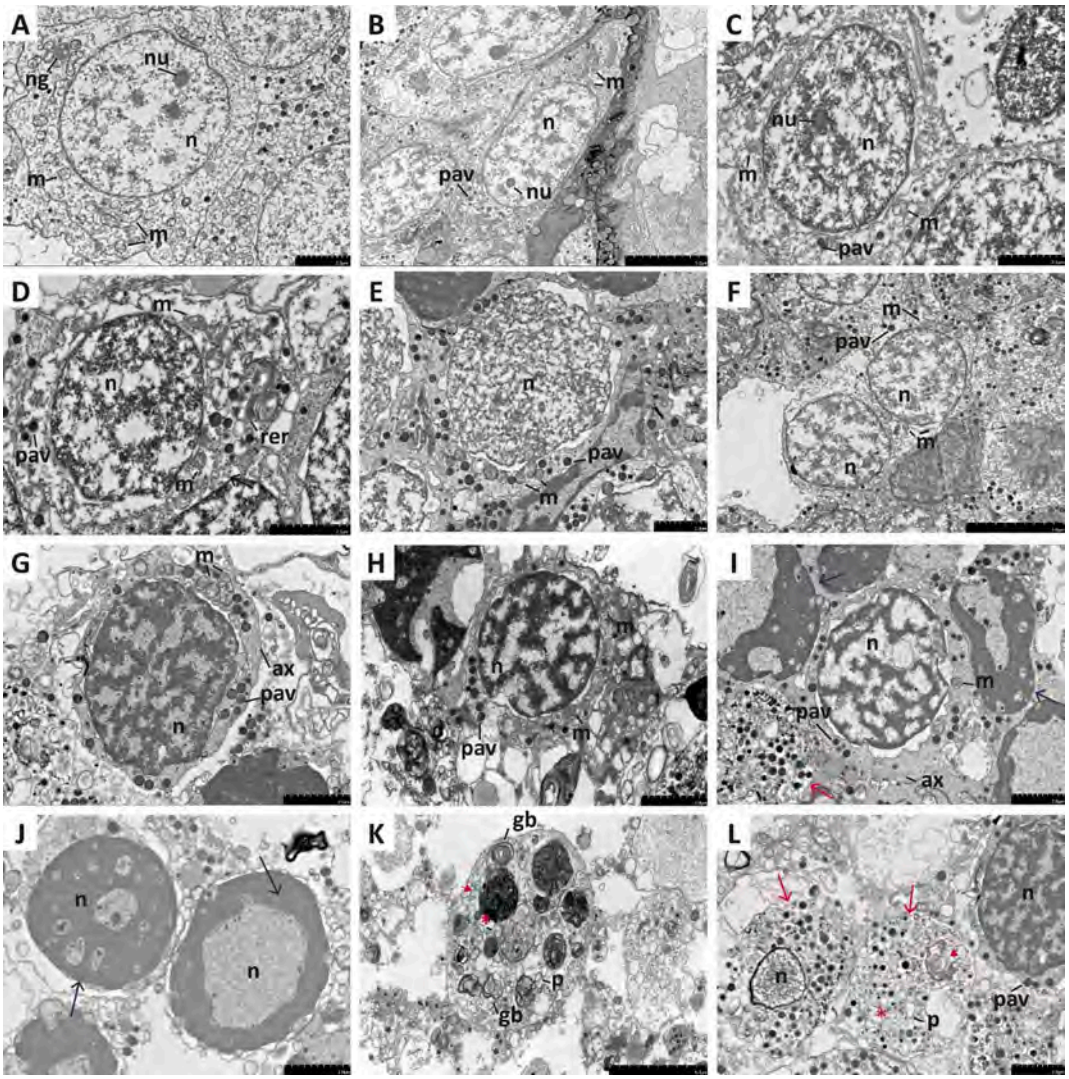

Fig. 5. Transmission electron micrographs of spermiogenesis in triploid *H. discus hannai*. A: spermatogonia, B: early primary spermatocytes, C–D: medium-term primary spermatocytes, E: late primary spermatocytes, F: dividing primary spermatocytes, G–H: secondary spermatocytes, I–J: apoptotic cells (blue arrow), K–L: autophagic cells (red arrow), n: nucleus, nu: nucleolus, ng: nuage, m: mitochondria, pav: proacrosomal vesicle, rer: rough endoplazmik reticulum, ax: axoneme, gc: Golgi complexes, p: phagophore, red asterisk: autophagosome, red arrowhead: autolysosome. (For interpretation of the references to colour in this figure legend, the reader is referred to the web version of this article.)

ELISA kit (Ann Arbor, Michigan, USA) according to the manufacturer's instructions. The resulting extracted samples were dissolved in ethanol and assay buffer and vortexed three times to ensure complete steroid solubility. Diluted standards, samples, conjugate antibody, wash solution, TMB substrate, and stop solution were successively added to a plastic microtiter plate coated with goat anti-rabbit IgG. The optical density of each well was measured at 450 nm using a microplate reader (Infunite M200 Pro, Tecan, Switzerland). The concentrations of samples were calculated from a standard curve plotted by a four-parameter logistic curve (4PLC) fitted with ELISA Calc (version 0.2) software. To assess the efficiency of extraction, known concentrations of E2 and T standards were added to pre-extracted homogenates. The percentages of recovery rate were 82.62 ± 7.02 % ($n = 3$, $R^2 = 0.998$) and 87.04 ± 5.85 % ($n = 3$, $R^2 = 0.998$) for E2 and T, respectively.

2.6. Data analysis

The normality and homoscedasticity of the data were validated via the Shapiro-Wilk and Levene's tests. The observed sex ratios (female: male) were tested against the 1:1 expected ratio using χ^2 tests. Student's *t*-tests (for normally distributed data with homogeneous variances) and Mann-Whitney *U* tests (non-normally distributed or heterogeneous variance) were used to analyze differences between ploidy levels for the following traits: (1) GBIn in different months, (2) GBIn and FMSI within the same gender, and (3) steroid values for specific stages. The above approach was also applied to comparing the differences in GBIn and FMSI between mean values for females and males at the same ploidy level. The degree of association between GBIn and FMSI was determined using linear regression and Spearman rank-correlation analyses. One-way ANOVA (normality and variance homogeneity) and independent-samples Kruskal-Wallis test (absence of normality or variance heterogeneity) were performed to examine the differences in the steroid concentrations between stages (ANOVA followed by Tukey's post hoc test). All of the statistical analyses were performed using the IBM SPSS (version 19) and R (version 4.1.0) software. The relevant data were presented as mean ± standard deviation, and the significance level for all of the analyses was set as $P < 0.05$.

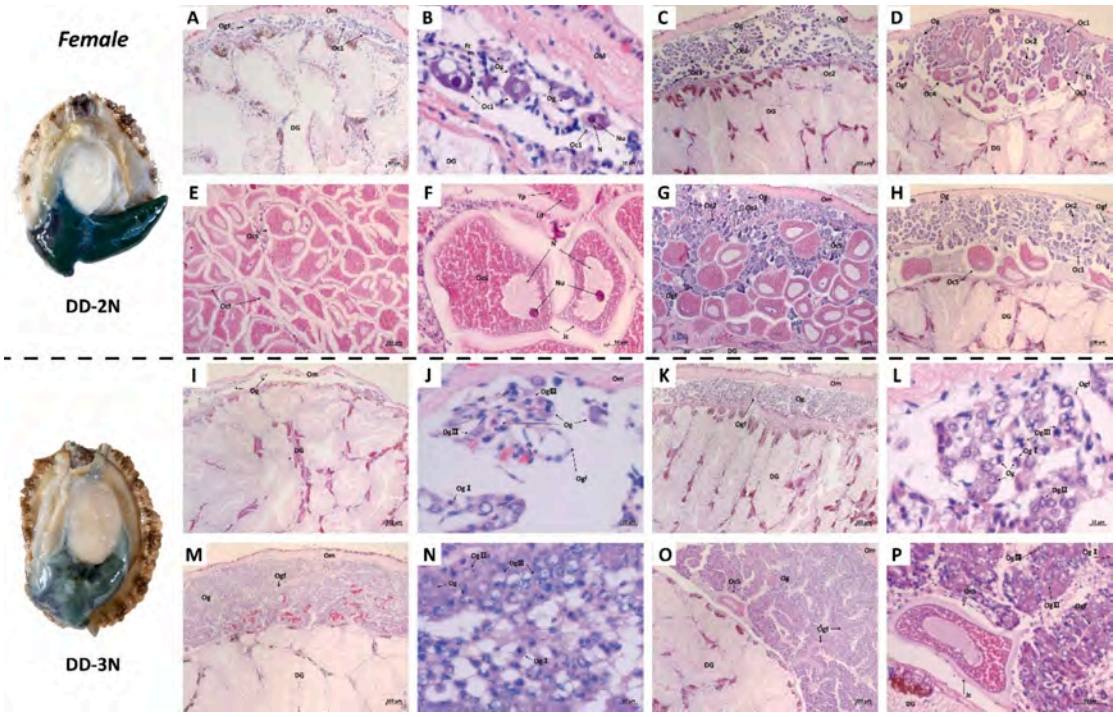

Fig. 6. Different stages of gonadal development in the females of diploid (DD 2 N) and triploid (DD 3 N) *H. discus hannai*. The inactive stage (A–B), early active stage (C), late active stage (D), ripe stage (E–F), spent stage (G) and degenerative stage (H) were derived from diploid ovarian development. The ovarian development of triploids comprised stage I (I–J), stage II (*K*−*L*), stage III (M–N), and stage IV (O–P). Og: oogonia, Oc1: stage I oocyte, Oc2: stage II oocyte, Oc3: stage III oocyte, Oc4: stage IV oocyte, Oc5: stage V oocyte, Og I: type I oogonia, Og II: type II oogonia, Og III: type III oogonia, N: nucleus, Nu: nucleolus, Ld: lipid droplet, Yp: yolk granule, Ogf: oogenic follicle, Om: ovarian outer membrane, DG, digestive gland.

3. Results

3.1. Characterization of gametogenesis

3.1.1. Oogenesis

Based on the changes in morphology, size, and vitellogenesis processes, female germ cells in *H. discus hannai* were divided into five stages inclusive of oogonia (Og), stage I oocytes (Oc1), stage II oocytes (Oc2), stage III oocytes (Oc3), stage IV oocytes (Oc4), and stage V oocytes (Oc5) (Figs. 1 and 2). The oogenesis of diploids was normal, possessing all of the germ cell types from the oogonia to the mature oocytes. Conversely, only oogonia and two types of oocytes (Oc2 and Oc5) were observed in triploid ovaries, although female triploids retained the capacity for accomplishing oogenesis. Multiple layers of arranged triploid oogonia (< 30 μm, slightly acidophilic and basophilic) were divided into three categories based on features of the nucleus under light microscopy (Fig. 1D): (1) type I oogonia (Og I), in which the nucleus was opaque and dense, and the borders of the nucleus and the cell membrane were sharply demarcated; (2) type II oogonia (Og II), in which deeply stained heterochromatin was attached to the inner side of the nuclear envelope of the nucleus (i.e., an inconspicuous nucleolus), and the cell membrane border was blurred in most cases. This cell type showed the highest similarity to the diploid oogonia under the light microscope. (3) type III oogonia (Og III), in which the nucleus with indistinct nuclear membrane boundaries contained condensed chromosomes, and most cells had an obscure cell edge. The three types of triploid oogonia with different nuclear characteristics were observed under the electron microscope, in which the cytoplasm contained subcellular structures in the form of mitochondria and dense aggregates (nuage). The cytological features of triploid oogonia that lacked a distinct nucleolus were similar to those of their diploid counterparts, surrounding the presence of narrow follicle cells (Fig. 2J and L). Triploid oogonia with a pronounced nucleolus lacked Golgi complexes in comparison to the corresponding diploid oogonia, whereas clusters of mitochondria were present in the ooplasm (Fig. 2K). The cellular characteristics of Oc2 and Oc5 in triploid abalone were comparable to those of diploids under light microscopy. The dominant characteristics of triploid mature oocytes (Oc5) enveloping the vitelline envelope were consistent with those of diploids, in which mitochondria, Golgi complexes, numerous lipid droplets, and abundant yolk granules were observed in the cytoplasm at this stage (Fig. 2N and O).

3.1.2. Spermatogenesis

There are five stages of male germ cells in *H. discus hannai*: spermatogonia (Sg), primary spermatocytes (Ps), secondary spermatocytes (Ss), spermatids (St), and spermatozoa (Sz) (Figs. 3 and 4). The spermatogenesis of diploids proceeded normally, with the gonads exhibiting all of the germ cell types from spermatogonia to spermatozoa. Early germ cells (Sg, Ps, and Ss) for spermatogenesis were observed in triploid testes under light microscopy. There were very few dividing spermatocytes in addition to a class of eosinophilic vacuole-like cells (inconspicuous nuclei) (Fig. 3D). The fundamental cytological traits of spermatogonia and primary spermatocytes of triploids were consistent with those of diploids, except for the reductions in the size and number of mitochondria in the cytoplasm of medium-term primary spermatocytes (Fig. 5). Late-dividing late primary spermatocytes (Fig. 5F) and secondary spermatocytes (Fig. 5G and H) containing an axoneme and variably sized mitochondria were present in triploid testes, without observation of spermatids and spermatozoa characterized by fusion of the proacrosomal vesicle to form an acrosome. Two cell populations with distinctive ultrastructural features were identified: (1) apoptotic spermatocytes, whose main features included cytoplasm condensation, condensed chromatin forming crescent-shaped masses on the inside of nuclear envelope, and budding of membranes (Fig. 5I and J), and (2) cells with autophagic vacuoles, where the cytoplasm was densely filled with phagophores (cup-shaped membranous elements), double-

Table 1
Descriptions of stages of ovarian development for diploid and triploid *Haliotis discus hannai*.

Diploid		Triploid	
Description	Cell types	Description	Cell types
Inactive stage (IN) Female early-stage cells (oogonia and basophilic homogeneous oocytes) are closely attached to the trabeculae, where oogonia are arranged in multiple layers near the capsular side.	Og, Oc1	**Stage I** Three types of oogonia are normally arranged in multiple layers or clusters near the capsular side in the follicles.	Og I, Og II, Og III
Early active stage (EA) The lumina of follicles develop with distinct branches. The follicles are filled with oogonia and heterogeneous oocytes, with oocytes arranged in grape-like clusters attached to the trabeculae.	Og, Oc1, Oc2	**Stage II** The lumina of follicles develop with branches. All oogonia form clusters and are attached to the trabeculae.	Og I, Og II, Og III
Late active stage (LA) The follicles are dominated by oogonia and heterogeneous oocytes, with both Oc3 (attached by a cytoplasmic stalk) and Oc4 (closer to the central area of the lumen) showing eosinophilic yolk granules. Some of the lumina concurrently have partially free mature oocytes in the center.	Og, Oc1, Oc2, Oc3, Oc4	**Stage III** Further development of the lumina of follicles is accompanied by thinning of the trabeculae. Most lumina are occupied by a large number of oogonia, and one or two oocytes are present in individual lumina in a minority of females.	Og I, Og II, Og III, Oc1, Oc2
Ripe stage (R) The follicles are larger, and the trabeculae become slimmer. Follicles are full of postvitellogenic oocytes (Oc4 and Oc5), and these are free in the lumen of the oogenetic compartment.	Oc4, Oc5	**Stage IV** The continuous process of female germ cell development is difficult to observe within the developing follicle. Most lumina of follicles are dominated by a large number of oogonia, and a few lumina contain individual mature oocytes free in the lumen. The area near the hepatopancreas side shows more broken connective tissue. The small number of oocytes at this stage makes it difficult to further identify and distinguish between maturation, spawning, and resorption in ovarian development.	Og I, Og II, Og III, Oc5
Spent stage (SP) Follicles gradually atrophy and contain undischarged oocytes (Oc5) and early-stage cells, with spaces in the follicles left by spawned mature oocytes.	Og, Oc1, Oc2, Oc5		
Degenerative stage (D) A few degenerated oocytes remain in the follicles, and the number of early oocytes arranged on the trabeculae is increased.	Og, Oc1, Oc2, Oc5		

membraned autophagosomes (containing undigested cytoplasmic material) and autolysosomes (single membrane-bound elements enclosing degraded organelles) (Fig. 5K and L). The eosinophilic vacuole-like cells observed under light microscopy may have resulted from apoptosis and autophagy. Cells with the cytological characteristics of spermatids and spermatozoa were not identified within the triploid testis.

3.2. Characterization of gonad development

3.2.1. Females

The ovarian development in a complete reproductive cycle of *H. discus hannai* was classified into six distinct stages depending on the follicle size and histological changes during oogenesis (Fig. 6 and Table 1). There were an inactive stage (IN), an early active stage (EA), a late active stage (LA), a ripe stage (R), a spent stage (SP), and a degenerative stage (D). Follicles of female diploids at the maturation stage were filled with mature oocytes, and all of the oogonia were capable of accomplishing oogenesis to form mature gametes. Ovarian development was abnormal in triploids, divided into four stages (stages I – IV) based on more detailed developmental features. The follicles of stage I and stage II were devoid of oocytes and were dominated by developing oogonia (Og I, Og II, and Og III). The follicles of most individuals in stage III contained large numbers of oogonia, and one or two previtellogenic oocytes (Oc1 and Oc2) were observed in the follicles of several females in this stage. In stage IV, connective tissue was present at the inner edges of the gonads, with a few mature oocytes (Oc5) visible in the minority of follicles. Stage IV had the highest relative abundance of mature gametes in the follicles and was the closest to the maturation stage of diploid females. Despite the presence of mature oocytes in female triploid ovaries, the minimal number of oocytes made it difficult to categorize stages relative to diploid maturation, spawning, and resorption.

3.2.2. Males

Testis development of *H. discus hannai* was classified into six stages (IN, EA, LA, R, SP, and D) characterized by follicle size and the progression of spermatogenesis (Fig. 7 and Table 2). Diploid male follicles at the maturation stage were filled with spermatozoa, indicating that the spermatogenic cells were prepared to differentiate into the next stage. Testis development of triploids with abnormal post-spermatogenesis was divided into four stages (stages I–IV). Stage I was characterized similarly to IN, with the trabeculae presenting the shape of clouds and attached spermatogonia. The spermatogenic cells within the follicles were centripetally arranged in stage II, in order from outside to inside, with spermatogonia, spermatocytes, and eosinophilic vacuole-like cells close to secondary spermatocytes. The follicles in stage III were contracted and occupied by the remaining strongly basophilic spermatocytes and some additional connective tissue. The degenerated follicles in stage IV were dominated by connective tissue and spermatogonia. Stage II most closely matched the maturation stage of diploid males, but no spermatozoa were visible throughout testis development of triploids.

3.3. Sex ratio

The sex proportion and sex ratio of diploids and triploids are shown in Table 3. Diploids only featured female and male individuals, while 8.95 % of unidentifiable individuals (undeveloped follicles or incomplete differentiation) were observed in triploids. The sex ratio (female: male) of both diploids and triploids followed the expected 1:1 ratio ($P > 0.05$).

3.4. Temporal distribution of gonadal development stages

There was a perceptible cyclical change in the gonadal development of diploids (Fig. 8). More than half of the diploids were in the initiation stage (IN) at the first time of sampling, and a minority reentered the reproductive cycle in December and the following February. The gonadal development of female and male diploids was not completely synchronous, with females showing a faster pace. Female diploids were primarily in the ripening and spawning stages in October, while males were mostly in the growing stage from October to December and attained sexual maturity next February (Fig. 8A). No cyclical pattern was observed in the gonadal development of triploid females, and 87.10 % of such individuals were in the period (stage I, stage II, and stage III) characterized by the absence of mature oocytes in the follicles (Fig. 8B). In contrast, the seasonal changes in gonadal development in triploid males were clearly distinguished by three distinct periods: a period of spermatogonia proliferation (stage I, June), a growing guiding period (stage II, August–October), and the remaining stages of development (stage III and stage IV, December–February). The nearest stages of

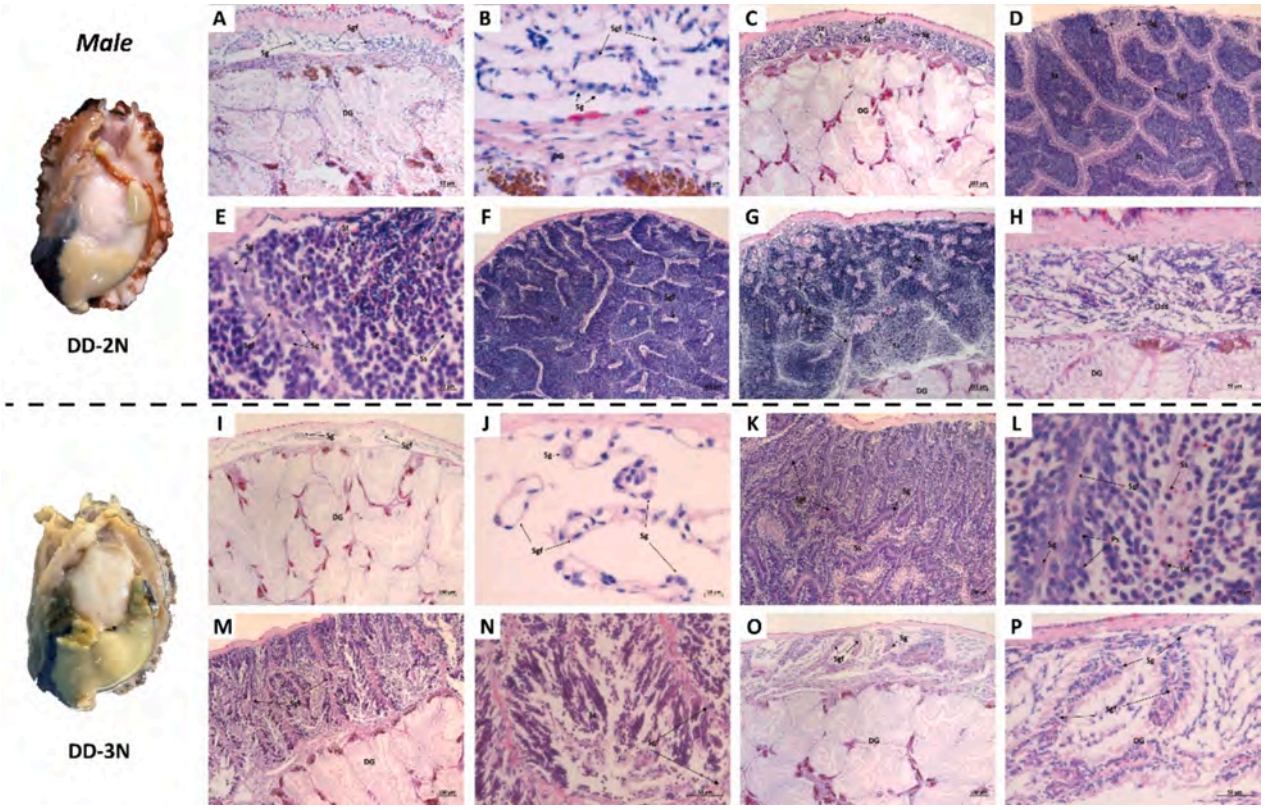

Fig. 7. Different stages of gonadal development in the males of diploid (DD 2 N) and triploid (DD 3 N) *H. discus hannai*. The inactive stage (A–B), early active stage (C), late active stage (D–E), ripe stage (F), spent stage (G) and degenerative stage (H) were derived from diploid testis development. The testis development of triploids comprised stage I (I–J), stage II (K–L), stage III (M–N) and stage IV (O–P). Sg: spermatogonia, Ps: primary spermatocytes, Ss: secondary spermatocytes, St: spermatids, Sz: spermatozoa, Uc: dividing spermatocytes, red arrow: vacuole-like cells, Sgf: spermatogenesis follicle. (For interpretation of the references to colour in this figure legend, the reader is referred to the web version of this article.)

triploid gonadal development to diploid maturity were stage IV in females and stage II in males. The percentage of triploid males in stage II (60.00 %) was higher than that of females in stage IV (12.90 %) throughout the observation period.

3.5. GBIn

The GBIn of diploids and triploids varied from 15.92 % to 88.75 % and 15.61 % to 50.24 % during the experimental period (Fig. 9). Both diploids and triploids showed trends where the GBIn first increased and then decreased. The GBIn (88.75 %) of diploids reached its highest value in October, when the gonadal development of most diploids was in the growing and maturation stages (LA and R). Over the same period, the GBIn of triploids was significantly lower than that of diploids ($P < 0.05$), with a higher discrete degree of GBIn (mean = 41.07 %, range = 86.71 %) in triploids. The GBIn of triploids (50.24 %, 56.61 % of diploids' peak) attained the highest level in December, when most triploid females and males were in stage III and stage II, respectively. Diploids and triploids entered terminal gonadal development the following February, when the GBIn of diploids remained higher than the triploids' peak and had a significantly greater average than that of triploids for the same period ($P < 0.05$).

3.6. Relationship among GBIn, FMSI, and gender

There were negative correlations between GBIn and FMSI in both diploids ($R = -0.18$, $P = 0.045$) and triploids ($R = -0.20$, $P = 0.035$) during the reproductive cycle (Fig. 10A). The FMSI declined significantly with increasing gonadal fullness.

The GBIn and FMSI values between different genders for the two populations are shown in Fig. 10B and C. In the same ploidy level, there were no significant differences in the two indices between the sexes of diploids ($P > 0.05$), whereas a higher value of FMSI (61.31 %) and a lower value of GBIn (22.56 %) were simultaneously present in triploid females ($P < 0.05$). Based on the same sex, there were no significant differences in GBIn or FMSI between diploid and triploid males, while triploid females had significantly higher levels of FMSI and GBIn in comparison to diploid females ($P < 0.05$).

3.7. Effective number of viable gametes in females

In the breeding season (October), the mature oocyte count per unit area of triploids (0.06 ± 0.17 count/mm^2) was significantly lower than that of diploids (47.31 ± 14.23 count/mm^2), representing 0.13 % that of diploids ($P < 0.05$).

3.8. Steroid concentrations

The dynamics of two steroid hormones during the reproductive cycle are represented in Fig. 11. The E2 contents of diploids fluctuated significantly with ovarian development, reaching peaks at the initiation stage (IN/D, 2.14 ng/g) and maturation stage (R, 1.33 ng/g), with the contents at both stages being significantly higher than those of the other developmental periods (EA/LA and SP) ($P < 0.05$). In triploids, the E2 concentrations of the female gonads showed no distinct variation throughout development, increasing to the highest value (1.29 ng/g) in stage IV (the presence of mature gametes in the follicles). A comparison of the E2 contents at similar gonadal developmental stages between diploids and triploids revealed that the hormone contents of stage IV triploid females were similar to that of the ovarian maturation stage (R)

Table 2
Descriptions of stages of testis development for diploid and triploid *Haliotis discus hannai*.

Diploid		Triploid	
Description	Cell types	Description	Cell types
Inactive stage (IN) The trabeculae are shown as a cloud in bulk with one or two layers of closely attached spermatogonia.	Sg	**Stage I** One or two layers of spermatogonia are located around the short and dilated trabeculae.	Sg
Early active stage (EA) The follicles have lumina and developed branches. The lumen is loaded with spermatogonia and a small number of spermatocytes (Ps and Ss, developed toward the lumen).	Sg, Ps, Ss, St, Sz	**Stage II** The follicles undergo further development and increase in size. Lumina of follicles are occupied by a large number of spermatogonia and primary spermatocytes. The lumina also contain very few dividing spermatocytes, and eosinophilic vacuole-like cells (inconspicuous nuclei) are present.	Sg, Ps, Ss
Late active stage (LA) The lumina become enlarged, and the extended trabeculae are thinner. The follicles contain all male germ cell types, especially a mass of strongly basophilic spermatids and spermatozoa. Spermatogonia, spermatocytes, spermatids, and spermatozoa are distributed in a centripetal pattern from the follicle walls to the lumen.	Sg, Ps, Ss, St, Sz		
Ripe stage (R) Follicles reach complete development, and the trabeculae become slimmer. The follicles are packed with strongly basophilic, centripetally arranged spermatozoa masses, while spermatogonia and spermatocytes are barely visible.	Sz		
Spent stage (SP) Follicles gradually atrophy and retain a loosened sperm mass. Small amounts of connective tissue and spermatogonia are present.	Sg, Sz	**Stage III** The follicles gradually contract and are filled with spermatocytes and centrally located eosinophilic vacuole-like cells. The vesicular connective tissue is significantly increased, and there are very few attached spermatogonia on the trabeculae.	Ss
Degenerative stage (D) A few residual spermatozoa remain in the testis. The trabeculae of empty follicles are shown as a cloud and accompanied by a small number of spermatogonia.	Sg, Sz	**Stage IV** The gonad lumen is collapsed, with abundant vesicular connective tissue and spermatogonia. Residual spermatogonia are found within the follicles in a few males.	Sg, Ss

Table 3
Number of female, male, and inactive abalone and the sex ratio among diploid (DD 2 N) and triploid (DD 3 N) *H. discus hannai*.

	Female	Male	Unidentifiable	Total	Sex ratio (F:M)	χ^2	*P* value
DD 2 N	73	73	0	146	1:1.00	0.00	1.000
DD 3 N	60	62	12	134	1:0.97	0.03	0.856

of diploids ($P > 0.05$). However, the E2 contents in the ovaries at the initiation stage (stage I/II) of triploids were significantly lower than those of diploids at a similar stage (IN/D) ($P = 0.001$), being only 32.20 % of the latter. T concentrations in both diploids and triploids were stable throughout the reproductive cycle ($P > 0.05$). There was no significant difference in T levels in the gonads during the initial stages (IN/D and stage I/II) of ovarian development between diploids and triploids ($P > 0.05$), and the same pattern was observed at the stages (R and stage IV) characterized by the highest relative abundance of mature gametes.

During testis development, the contents of both hormones in diploid testes fluctuated with development, first increasing and then decreasing, with a trend in which the T levels of the maturation stage were significantly higher than those in other developmental stages ($P < 0.05$). In triploids, the levels of both hormones in the testes exhibited an upward trend throughout gonad development, reaching their highest values (E2: 2.50 ng/g, T: 2.54 ng/g) during stage III. Examination of the hormone expression levels in the gonads of corresponding individuals at the late phases of differentiation in spermatogenesis found that the levels of E2 and T during the growth phase (EA/LA) of diploid testes were similar to those of the corresponding stage (stage II) in triploids ($P > 0.05$). In contrast, the expression levels of E2 ($P = 0.001$) and T ($P = 0.014$) in the triploid gonads at the stagnant stage (stage II) of spermatogenesis were significantly lower than those of diploids in the maturation stage (R).

4. Discussion

One additional chromosome can have varying degrees of impact on the gametogenesis of triploid fish and shellfish. In this study, triploid abalone were shown to have abnormalities in oogenesis. Triploid female *H. discus hannai* were able to produce mature oocytes; along with the absence of cell types corresponding to diploid female germ cells, this suggests that the occurrence of a very few previtellogenic oocytes appeared to be random, and most oogonia lacked the potential for further differentiation. The substantial retardation of oogenesis observed in the triploid *H. discus hannai* was distinct from the functional sterility of the female triploid *H. rubra* (Liu et al., 2009) and lion's paw scallop *Nodipecten subnodosus* (Maldonado-Amparo et al., 2004; Galindo-Torres et al., 2022). The low fecundity due to the reduced number of oocytes was similar to previous findings in the chemical triploid Catarina scallop *Argopecten ventricosus* (Maldonado-Amparo and Ibarra, 2002), the β females of mated triploid *C. gigas* (Jouaux et al., 2010; Yang et al., 2022b), and oligo females of the mated triploid *C. virginica* (Matt and Allen, 2021). This phenomenon of arrested oogenesis is typically manifested as an accumulation of abnormal oogonia and an extremely reduced number of mature oocytes in the triploid follicles. Changes in the density of chromosomes in the nuclei were observed in abnormal oogonia (β gonia) of the two oysters mentioned above, where the β gonia of triploid *C. gigas* was further considered to have possible mitotic locking (Jouaux et al., 2010) or abnormal proliferation (Yang et al., 2022a; Yang et al., 2024). Abnormal oogonia in the ovaries of triploid *H. discus hannai* exhibited unique and differentiated histological features, possibly reflecting differences in their developmental potential. Oogonia in diploids typically differentiate normally, meaning that those with distinct single-cell characteristics are likely to be at the same stages of proliferation and differentiation. Nonetheless, the developmental potential of female germ cells in most triploid mollusks tends to converge to that of diploids, with females producing a considerable number of mature gametes, especially in oysters. The relative fecundity of female triploid *C. gigas* was 5.23 %–13.4 % of that of a normal diploid, with α female oysters producing a significant number of oocytes (Gong et al., 2004; Suquet et al., 2016; Yang et al., 2022b). In contrast, the effective number of viable gametes of female triploid *H. discus hannai* during the breeding season was only 0.13 % of that observed in diploids. In addition to interspecific differences, the patterns of gonadal development and gametogenesis in triploids also depend on the approaches used for

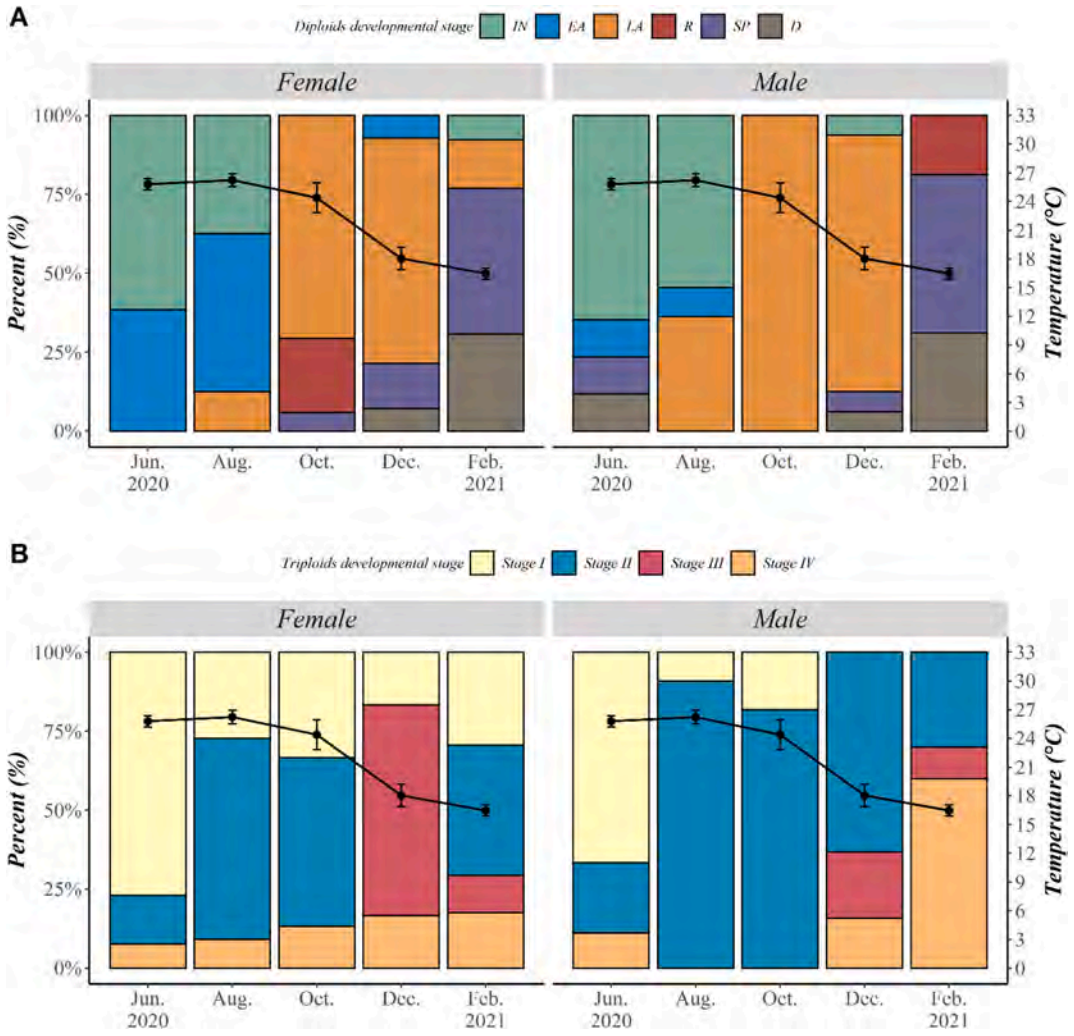

Fig. 8. Frequency of gonad developmental stages in diploid (A) and triploid (B) *Haliotis discus hannai* and monthly variation of the water temperature in the sampling area. The gonad development of diploids was divided into six stages: IN: inactive stage, EA: early active stage, LA: late active stage, R: ripe stage, SP: spent stage, D: degenerative stage. The gonad development of triploids was assigned to four stages (stage I, stage II, stage III, and stage IV).

production and the timing of sampling (i.e., age and season) (Lahnsteiner et al., 2021; Matt and Allen, 2021). However, the breeding strategy for all-triploid shellfish currently depends on the development of triploid-tetraploid breeding technology (Yang et al., 2019). A primary challenge in producing tetraploids is the limited availability of mature oocytes from triploid females. The significant decline in female fecundity, particularly in the quantity of mature gametes, in triploid *H. discus hannai* may impede the effective implementation of all-triploid abalone breeding programs.

The development of spermatogenesis in male triploids of fish and shellfish is more complex. Theoretically, the sterility resulting from random segregation of trivalents during meiosis in male germ cells of triploids is commonly manifested as interference with the second meiotic division and the differentiation of spermatocytes (Piferrer et al., 2009). The disruption of spermatogenesis in male triploid *H. discus hannai* was characterized in our study in the form of male germ cells becoming arrested at the spermatogonia stage. The sterility pattern of male triploid *H. discus hannai* was more aligned with gametic sterility (normal size gonads but abnormal spermatogenesis) than gonadic sterility or zygotic sterility (Chevassus, 1983). Gametic sterility has been previously observed in male triploids of the European sea bass *Dicentrarchus labrax* (Peruzzi et al., 2004), *N. subnodosus* (Maldonado-Amparo et al., 2004), *M. edulis* (Brake et al., 2004), and the Peruvian scallop *Argopecten purpuratus* (Lohrmann and Von Brand, 2005), where spermatogenesis is typically arrested at the spermatocyte or spermatid stage. The description of developmental processes of male germ cells in male triploid *H. discus hannai* has been inconsistent in previous studies. Initial studies showed that spermatogenesis in triploid *H. discus hannai* was arrested at the spermatid stage (malformation of spermatids) (Li et al., 2004; Yan et al., 2005). In the study of Jee et al. (2013), 25 % of male triploids in the spawning experiment produced spermatozoa that were significantly smaller and incapable of fertilizing diploid eggs. Kim et al. (2019) reported that a significant number of secondary spermatocytes were present in the testis of triploid abalone without observing spermatids or spermatozoa. The underlying reasons for this variation in spermatogenesis remain unclear, but it may be linked to the tissue ploidy levels and the age of the triploid individuals. Other observations of triploid Salmonidae support the hypothesis that the number of functional gametes in the testes of triploids varies with age (Lahnsteiner et al., 2021). In addition, the eosinophilic vacuole-like cells within the testicular follicles observed under light microscopy could be germ cells that have undergone apoptosis or autophagy. Apoptosis appears in triploids as a mechanism for the maintenance of the internal environment to eliminate residual, unknown, and damaged germ cells and to block the developmental maturation of germ cells with an abnormal number of chromosomes, as reported in *S. maximus* (Cal et al., 2010) and *C. gigas* (Chen et al., 2024).

The reproductive capacity of triploid shellfish is restricted, implying

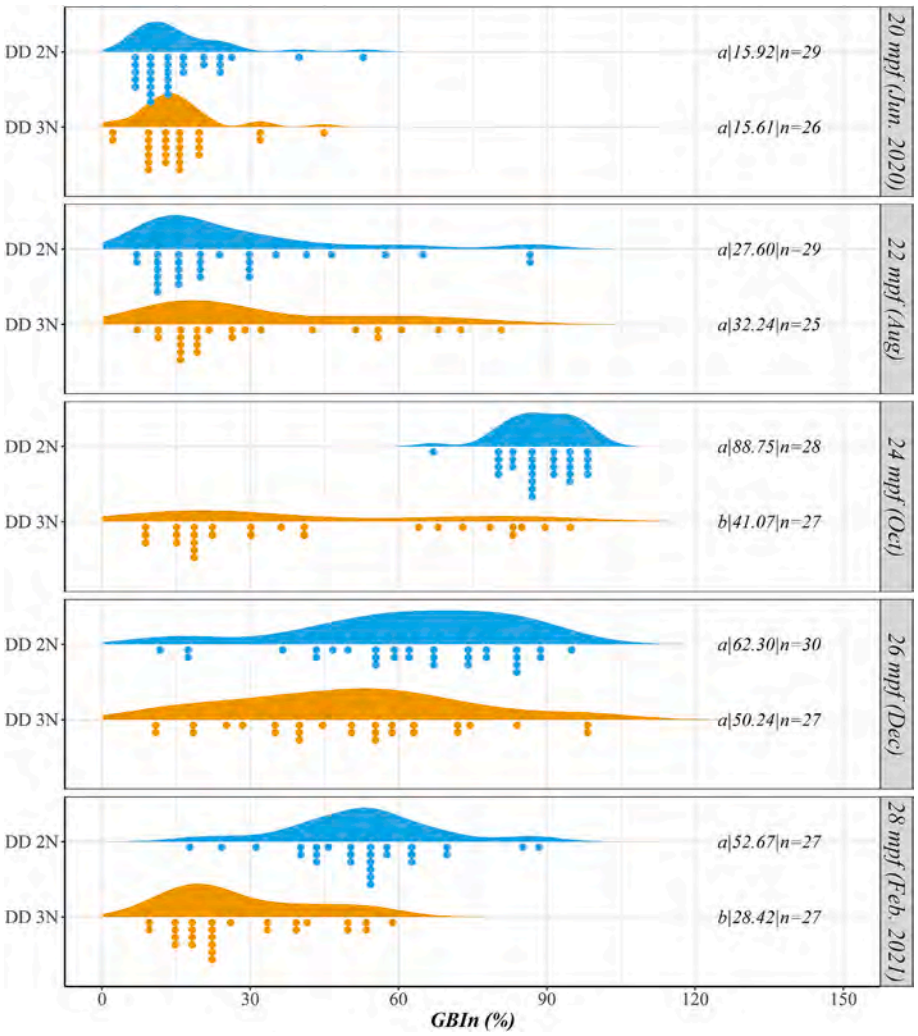

Fig. 9. Gonad bulk index (GBI_n) of diploids (DD 2 N) and triploids (DD 3 N) *H. discus hannai* over time. Different lowercase letters indicate significant differences between different ploidy at the same month ($P < 0.05$).

that the classification system for diploids with normal gonadal development may not be fully applicable to triploids with typical differences in gonadal development. In triploid *C. gigas*, gametogenesis followed two patterns: (1) the α-pattern, corresponding to individuals with orderly completion of gametogenesis and production of abundant mature gametes, and (2) the β-pattern, where individuals with locked gametogenesis produced only a few mature gametes (Jouaux et al., 2010). Gonadal development of triploid *C. gigas* was further categorized into female α (β gonia and many mature oocytes), female β (β gonia and scarcely any oocytes), male (a few spermatids), hermaphrodite I (β gonia, oocytes, and spermatogenic cells), and hermaphrodite II (oocytes and spermatogenic cells) based on the types of germ cells within the follicles (Yang et al., 2022b). For triploid *C. virginica*, the gonadal development was classified based on the types of gonia, with individuals presenting α gonia developing as males, and individuals presenting β gonia developing as females, oligo females, and virilescent females (Matt and Allen, 2021). Gonadal development in triploid *H. discus hannai* differs markedly from that in oysters, with developmental retardation being more homogeneous within the same sex. The above classification system does not include the correspondence among the stages of gonad development in diploids and triploids. In the present study, the division criteria specifically for gonadal development in triploid *H. discus hannai* were applicable to the cyclical observation of gonadal development, resulting in an effective assessment of reproductive potentiality in triploids. This division criterion is currently restricted by sample size and is most applicable to individuals from natural breeding environments. Moreover, 87.10 % of female triploid *H. discus hannai* were in the stages (stage I, stage II, and stage III) characterized by abnormal oogonia in the follicles during the complete reproductive cycle, indicating a higher proportion and a more homogenous pattern of retarded ovarian development in female triploids.

Differences in impaired gonadal development between the genders also affect the relative proportions of the edible portion in most triploid aquatic animals. This phenomenon was first noted in triploid fishes, as exemplified by the triploid barfin flounder *Verasper moseri*, where female triploids were sterile and demonstrated a lower gonadosomatic index and higher relative proportions of various body parts during the spawning period, suggesting that the advantage of female triploids was due to their sterility (Mori et al., 2006). Triploid striped catfish *Pangasianodon hypophthalmus* exhibited permanent sterility, accompanied by significant increases in fillet yield and quality, resulting in a 17.8 %–23.3 % increase in the percentage of fillets as well as an elevated protein nutritional value (comprising protein, fat, and nitrogen-free extract) (Carman et al., 2022). In addition, in the blacklip abalone *H. rubra*, male triploids produced a similar sized gonad to diploids and had a lower FMSI than female diploids, meaning that the energy consumed by gonad development remained a constraint on somatic growth for male triploids, whereas female triploids exhibited a significant reduction in gonadal development, suggesting that the increase in FMSI in triploid *H. rubra* was primarily attributed to females (Liu et al., 2009). In the

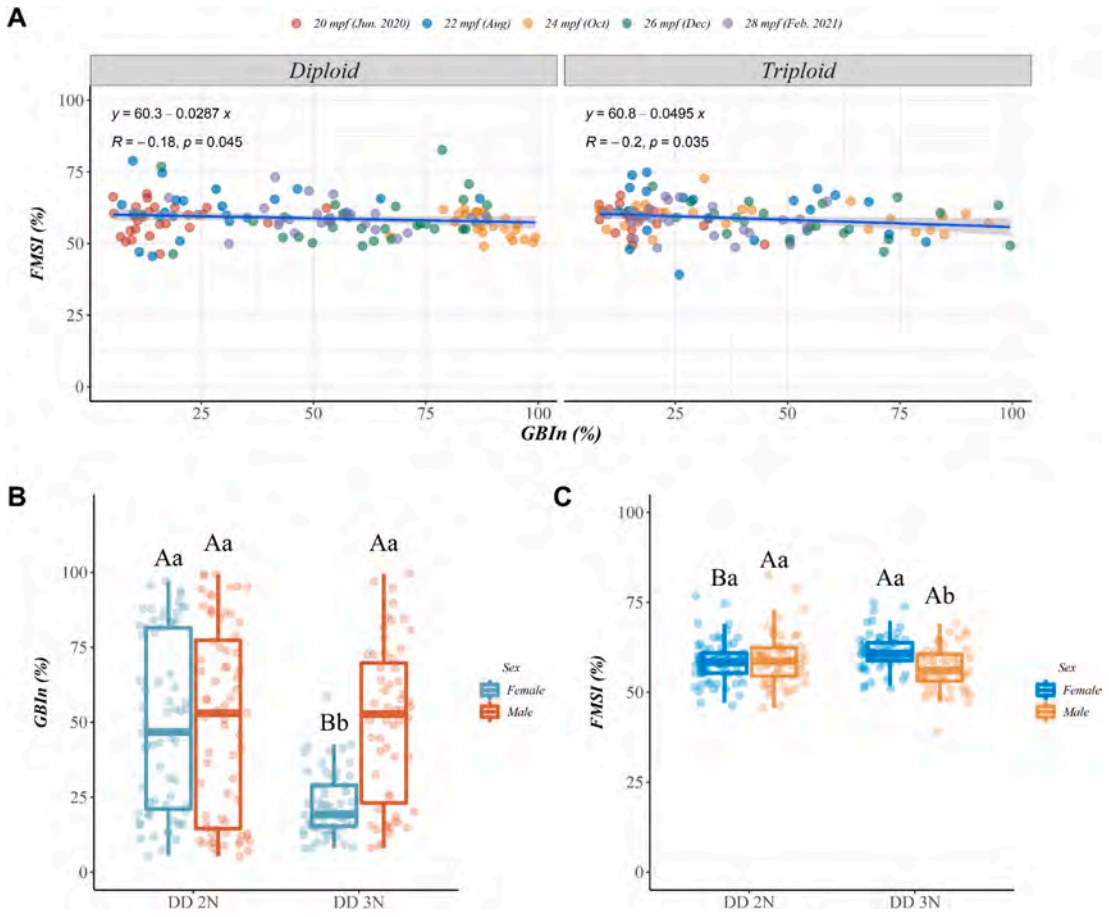

Fig. 10. Relationships among the gonad bulk index (GBI_n), the foot muscle-soft tissue index (FMSI), and gender in diploid (DD 2 N) and triploid (DD 3 N) *H. discus hannai*. A: correlation analysis of GBIn and FMSI in diploids and triploids, B: GBIn and FMSI of male and female diploids, C: GBIn and FMSI of male and female triploids. Different lowercase letters indicate significant differences between different genders at the same ploidy level, while different capital letters indicate significant differences between ploidy in the same sex ($P < 0.05$).

present study, the gonad was significantly reduced in triploid *H. discus hannai*, especially in females with low gonadal fullness and higher FMSI (4.60 % higher than diploid females). Combined with the negative correlation between gonadal fullness and FMSI in *H. discus hannai*, these results further support the hypothesis that the growth advantage of triploids may be attributed to energy reallocation due to sterility. Since the size of the foot muscles is the primary factor in the economic value of the individual, female abalone within triploid populations may have commercial advantages. To meet the production demands of individuals with higher carcass value and sterility characteristics, researchers have combined artificial triploid induction with the techniques of gynogenesis and sex reversal, resulting in the production of all-female triploids (sterile and demonstrating rapid growth) (Dunham, 2011). All-female triploid salmonids have been granted for commercial application in several countries and regions (Benfey, 2016). In addition, The FMSI of triploids did not differ from that of diploids during reproductive seasons, perhaps being influenced by the presence of males within the triploid population.

Vertebrates have a highly conserved hypothalamic-pituitary-gonadal (HPG) reproductive control system, whereas the neuroendocrine control of most mollusks is primarily composed of ganglia and a reproductive gland (gonad) that serves to regulate reproductive development (Sakai et al., 2020). In the present study, there were differences in the fluctuations of E2 and T levels within the gonads of triploids and diploids, primarily in the form of deficiencies in hormone levels at specific stages. In the initial stages of gonadal development, the levels of E2 were significantly reduced in triploid females to only 32.20 % of those in diploid females. Combined with the retardation of oogenesis in triploid *H. discus hannai*, this suggests that the low levels of E2 may only be able to support the development of a restricted number of oogonia into oocytes. Similar results have been observed in triploid yellowtail flounder *Limanda ferruginea*, with comparable characteristics of ovarian retardation (Manning et al., 2004). The sterility of triploid female rainbow trout has also been implicated as possibly being related to abnormal fluctuations in sex steroids, suggesting that high estrogen levels have a critical role in maintaining normal differentiation and development of the ovary (Xu et al., 2016). Likewise, the levels of E2 and T were decreased in the testes of sterile male triploid *H. discus hannai* compared to those of mature male diploids, and the testes of triploids during this stage were filled with developing male germ cells (spermatogonia and spermatocytes), indicating that the neuroendocrine control of male triploids may have remained partially functional. This was also suggested by a study of triploid grass puffer *Takifugu niphobles* (Hamasaki et al., 2013). Triploid olive flounder *Paralichthys olivaceus* with severely inhibited gonadal development also showed significant differences in sex steroid hormones in the ovary and testis (Wu et al., 2023). Abnormal development of the gonads in triploid fish and shellfish may be associated with insufficient functional steroid biosynthesis. Conversely, in natural triploid gibel carp *C. gibelio,* two sexes that produce mature gametes, changes in hormone concentrations were influenced mainly by the reproductive phase, rather than by ploidy (Przybyl et al., 2022).

In conclusion, our study indicates that the triploid of *H. discus hannai* shows disrupted gonadal development, reduced gonadal fullness, lower effective numbers of viable gametes, and decreased steroid hormone

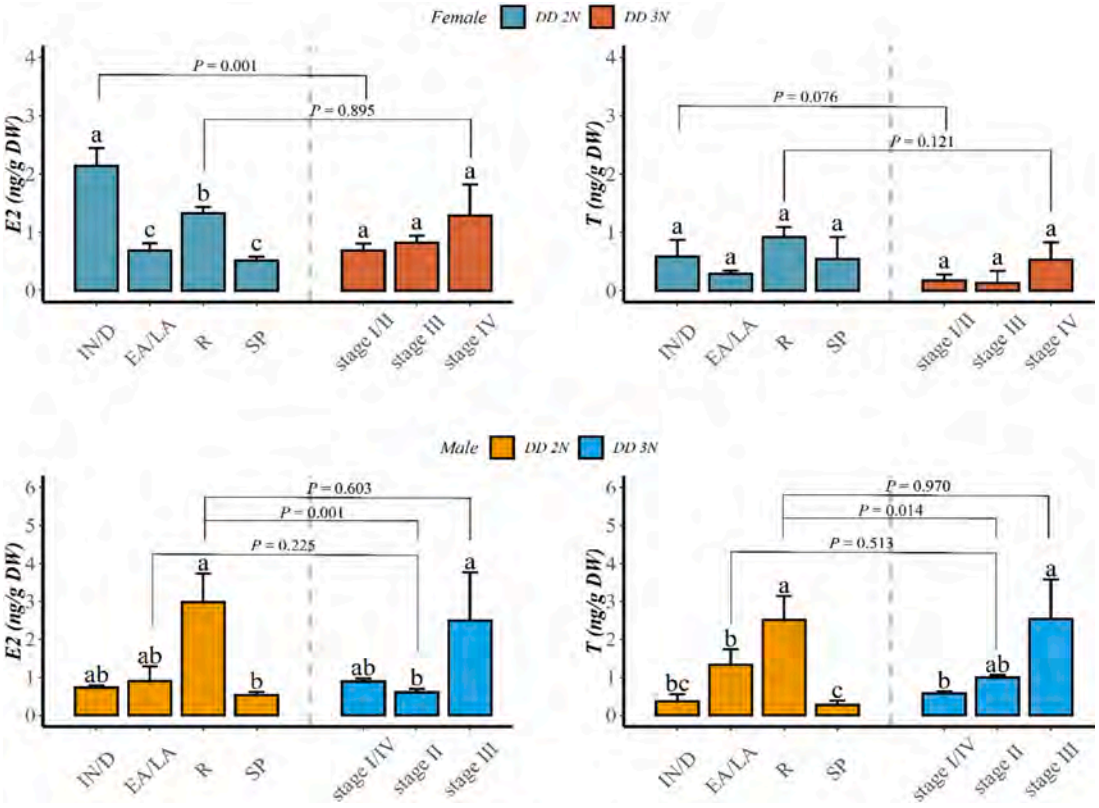

Fig. 11. Variation in estradiol-17β (E2) and testosterone (T) concentrations (ng/g dry weight) in different stages of gonadal development in diploid (DD 2 N) and triploid (DD 3 N) *H. discus hannai*. Gonadal contents of E2 and T in diploid females and males were examined in the following stages: IN/D: inactive stage and degenerative stage, EA/LA: early active stage and late active stage, R: ripe stage, SP: spent stage. Gonadal contents of E2 were measured in triploid females at stage I/II (stage I and stage II), stage III, and stage IV. The T concentrations in the gonads of triploid males were quantified at stage I/IV (stage I and stage IV), stage II and stage III. Bars represent means ± standard deviation (n = 3). Different lowercase letters indicate significant differences between different developmental stages at the same ploidy level ($P < 0.05$).

levels (stage-specific). Triploid females produced very few mature oocytes and had developing follicles occupied by large numbers of oogonia, while spermatogenesis in triploid males arrested in the spermatocyte stage, and the developing testis contained apoptotic and autophagic germ cells. A more precise set of division criteria of gonadal development in triploid *H. discus hannai* was also established. Furthermore, certain negative effects of gonadal development on meat yield were confirmed in both diploid and triploid *H. discus hannai*, where female triploids exhibited a significant decrease in gonadal fullness along with a significant increase in meat yield, suggesting that altered meat yield in triploids was associated with disruption of gonadal development, and that the saved energy from reduced reproductive investment could be more concentrated on body growth. The findings from this study provide references for the implementation of subsequent breeding strategies for triploid *H. discus hannai*, especially tetraploid breeding with triploid females as the parent stock. Further research should focus on the intrinsic regulatory mechanisms underlying gonadal changes in triploid abalones, particularly in terms of genetic changes and reproductive endocrinology.

CRediT authorship contribution statement

Yi Wang: Writing – review & editing, Writing – original draft, Visualization, Software, Funding acquisition, Formal analysis, Data curation. **Jianpeng Zhang:** Methodology, Investigation. **Yang Gan:** Methodology, Investigation. **Yexin Chen:** Resources. **Weiwei You:** Writing – review & editing, Investigation. **Xuan Luo:** Writing – review & editing, Validation, Supervision, Investigation. **Caihuan Ke:** Supervision, Resources, Funding acquisition, Conceptualization.

Declaration of competing interest

The authors declare that there is no conflict of interest.

Acknowledgements

This work was supported by grants from National Natural Science Foundation of China (No. 32172961 and 32403007), Fujian Provincial S & T Project (2024N3008), Postdoctoral Fellowship Program of CPSF (No. GZC20231423), China Postdoctoral Science Foundation (No. 2023M742928), Earmarked Fund for CARS (CARS-49), Independent Research Project of State Key Laboratory of Mariculture Breeding, and Outstanding Postdoctoral Scholarship of State Key Laboratory of Mariculture Breeding. We sincerely thank Jinwei Ke, Miaoqin Huang, Luming Yao, Qizhen Xiao, Yawei Shen, Mingcan Zhou for their kind help during this study.

Data availability

Data will be made available on request.

References

Apisawetakan, S., Thonckukiatkul, A., Wanichanon, C., Linthong, V., Kruatrachue, M., Upatham, E.S., Poomthong, T., Sobhon, P., 1997. The gametogenic processes in a tropical abalone, *Haliotis asinina* Linnaeus. J. Sci. Soc.Thail. 23, 225–240.

Arai, K., Okumura, S., 2013. Aquaculture-oriented genetic researches in abalone: current status and future perspective. Afr. J. Biotechnol. 12 (26), 4044–4052. https://doi.org/10.5897/AJB12.2178.

Benfey, T.J., 2016. Effectiveness of triploidy as a management tool for reproductive containment of farmed fish: Atlantic salmon (*Salmo salar*) as a case study. Rev. Aquac. 8 (3), 264–282. https://doi.org/10.1111/raq.12092.

Brake, J., Davidson, J., Davis, J., 2004. Field observations on growth, gametogenesis, and sex ratio of triploid and diploid *Mytilus edulis*. Aquaculture 236 (1), 179–191. https://doi.org/10.1016/J.AQUACULTURE.2003.09.016.

Brianik, C.J., Allam, B., 2023. The need for more information on the resistance to biological and environmental stressors in triploid oysters. Aquaculture 577, 739913. https://doi.org/10.1016/j.aquaculture.2023.739913.

Cal, R.M., Vidal, S., Gomez, C., Alvarez-Blazquez, B., Martinez, P., Piferrer, F., 2006. Growth and gonadal development in diploid and triploid turbot (*Scophthalmus maximus*). Aquaculture 251 (1), 99–108. https://doi.org/10.1016/j.aquaculture.2005.05.010.

Cal, R., Terrones, J., Vidal, S., Martinez, P., Piferrer, F., 2010. Differential incidence of gonadal apoptosis in triploid-induced male and female turbot (*Scophthalmus maximus*). Aquaculture 307 (3–4), 193–200. https://doi.org/10.1016/j.aquaculture.2010.07.020.

Carman, O., Hartami, P., Ibrahim, Y., Nasrullah, H., Alimuddin, Soelistyo Wati, D.T., Zairin Jr., M., Rahman, 2022. Reproduction, growth, fillet proportion and proximate analysis of tetraploid X diploid derived striped catfish (*Pangasianodon hypophthalmus*) triploid. AACL Bioflux. 15 (2), 744–757. https://doi.org/10.3897/aab.15.744.

Carman, O., Mukti, A.T., Zairin Jr., M., Alimuddin, 2023. Reproductive performances of triploid male and female Nile tilapia *Oreochromis niloticus* (Linnaeus, 1758) at different ages. Biodiversitas: J. Biol. Divers. 24 (8).

Chen, C., Yu, H., Li, Q., Kong, L., Liu, S., Xu, C., 2024. Examination of the effects of impaired spermatogenesis on sterility in triploid oysters (*Crassostrea gigas*), and implications for commercial aquaculture. Aquaculture 587, 740787. https://doi.org/10.1016/j.aquaculture.2024.740787.

Chevassus, B., 1983. Hybridization in fish. Aquaculture 33 (1), 245–262. https://doi.org/10.1016/0044-8486(83)90405-2.

China Bureau of Fisheries, 2024. China Fisheries Yearbook in 2024. Agricultural Press of China, Beijing, China.

Chung, E.Y., Ko, C.H., Kang, H.W., Choi, K.H., Jun, J.C., 2008. Ultrastructure of oocytes during oogenesis and oocyte degeneration associated with follicle cells in female *Sinonovacula constricta* (BIVALVIA: PHARIDAE) in Western Korea. Anim. Cells. Syst. 12 (4), 313–319. https://doi.org/10.1080/19768354.2008.9647187.

Das, S., 2014. Chapter 29 - biotechnological exploitation of marine animals. In: Verma, A.S., Singh, A. (Eds.), Animal Biotechnology. Academic Press, San Diego, pp. 541–562.

Dunham, R.A., 2011. Aquaculture and Fisheries Biotechnology: Genetic Approaches.

FAO, 2024. FAO Yearbook. Fishery and Aquaculture Statistics 2024, Rome.

Franco, A., Berthelin, C.H., Goux, D., Sourdaine, P., Mathieu, M., 2008. Fine structure of the early stages of spermatogenesis in the Pacific oyster, *Crassostrea gigas* (Mollusca, Bivalvia). Tissue Cell 40 (4), 251–260. https://doi.org/10.1016/j.tice.2007.12.006.

Galindo-Torres, P., Abreu-Goodger, C., Llera-Herrera, R., Escobedo-Fregoso, C., García-Gasca, A., Ibarra, A.M., 2022. Triploid-induced complete sterility in the scallop *Nodipecten subnodosus* might be triggered by an early and sustained DNA damage response. Aquaculture 559, 738422. https://doi.org/10.1016/j.aquaculture.2022.738422.

Gao, X., Zhang, M., Luo, X., You, W., Ke, C., 2022. Transitions, challenges and trends in China's abalone culture industry. Rev. Aquac. https://doi.org/10.1111/raq.12769.

Gong, N., Yang, H., Zhang, G., Landau, B.J., Guo, X., 2004. Chromosome inheritance in triploid Pacific oyster *Crassostrea gigas* Thunberg. Heredity 93 (5), 408–415. https://doi.org/10.1038/sj.hdy.6800517.

Haffray, P., Bruant, J.S., Facqueur, J.M., Fostier, A., 2005. Gonad development, growth, survival and quality traits in triploids of the protandrous hermaphrodyte gilthead seabream *Sparus aurata* (L.). Aquaculture 247 (1–4), 107–117. https://doi.org/10.1016/j.aquaculture.2005.02.037.

Hamasaki, M., Takeuchi, Y., Miyaki, K., Yoshizaki, G., 2013. Gonadal development and fertility of triploid grass puffer *Takifugu niphobles* induced by cold shock treatment. Mar. Biotechnol. 15 (2), 133–144. https://doi.org/10.1007/s10126-012-9470-3.

Jee, Y., Nam, B.H., Lee, J., Chang, Y., 2013. Maturity and spawning of the triploid pacific abalone, *Haliotis discus hannai*. Kor. J. Malacol. 29. https://doi.org/10.9710/kjm.2013.29.2.105.

Jouaux, A., Heude-Berthelin, C., Sourdaine, P., Mathieu, M., Kellner, K., 2010. Gametogenic stages in triploid oysters *Crassostrea gigas*: irregular locking of gonial proliferation and subsequent reproductive effort. J. Exp. Mar. Biol. Ecol. 395(1–2), 162–170. doi: https://doi.org/10.1016/j.jembe.2010.08.030.

Kim, E.J., Kim, S.J., Park, C.J., Nam, Y.K., 2019. Characterization of testis-specific serine/threonine kinase 1-like (TSSK1-like) gene and expression patterns in diploid and triploid Pacific abalone (*Haliotis discus hannai*; Gastropoda; Mollusca) males. PLoS ONE 14 (12). https://doi.org/10.1371/journal.pone.0226022.

Lahnsteiner, F., Lahnsteiner, E., Kletzl, M., 2021. Age and species related differences in gonad development of triploid Salmonidae. J. Appl. Aquac. 33 (3). https://doi.org/10.1080/10454438.2020.1760993.

Lee, K., 2008. Ultrastructural studies of oogenesis and oocyte degeneration in female *Ruditapes philippinarum* (Bivalvia: Veneridae) from Gomso Bay, Korea. Develop. Reprod. 12 (1), 41–49.

Li, X., Yan, S., Zhang, G., Wang, Z., 2004. The biology of gonadial development of triploidy abalone (*Haliotis discus hannai*). Oceanol. Et. Limnol. Sin. 01, 84–88.

Liu, W., Heasman, M., Simpson, R., 2009. Growth and reproductive performance of triploid and diploid blacklip abalone, *Haliotis rubra* (leach, 1814). Aquac. Res. 40 (2), 188–203. https://doi.org/10.1111/j.1365-2109.2008.02082.x.

Lohrmann, K.B., Von Brand, E., 2005. Histological study of gonads in triploid, scallops, *Argopecten purpuratus*. J. Shellfish Res. 24 (2), 369–375.

Maldonado-Amparo, R., Ibarra, A.M., 2002. Comparative analysis of oocyte type frequencies in diploid and triploid catarina scallop (*Argopecten ventricosus*) as indicators of meiotic failure. J. Shellfish Res. 21 (2), 597–603. https://doi.org/10.1046/j.1365-2761.2002.00412.x.

Maldonado-Amparo, R.O., Ramirez, J.L., Ávila, S., Ibarra, A.M., 2004. Triploid lion-paw scallop (*Nodipecten subnodosus* Sowerby); growth, gametogenesis, and gametic cell frequencies when grown at a high food availability site. Aquaculture 235 (1–4), 185–205. https://doi.org/10.1016/j.aquaculture.2003.12.014.

Manning, A.J., Burton, M.P.M., Crim, L.W., 2004. Reproductive evaluation of triploid yellowtail flounder, *Limanda ferruginea* (Storer). Aquaculture 242 (1–4), 625–640. https://doi.org/10.1016/j.aquaculture.2004.06.012.

Matt, J.L., Allen, S.K., 2021. A classification system for gonad development in triploid *Crassostrea virginica*. Aquaculture 532, 735994. https://doi.org/10.1016/j.aquaculture.2020.735994.

Mori, T., Saito, S., Kishioka, C., Arai, K., 2006. Aquaculture performance of triploid barfin flounder *Verasper moseri*. Fish. Sci. 72 (2), 270–277. https://doi.org/10.1111/j.1444-2906.2006.01148.x.

Murray, D.S., Kainz, M.J., Hebberecht, L., Sales, K.R., Hindar, K., Gage, M.J.G., 2018. Comparisons of reproductive function and fatty acid fillet quality between triploid and diploid farm Atlantic salmon (*Salmo salar*). R. Soc. Open Sci. 5 (8). https://doi.org/10.1098/rsos.180493.

Najmudeen, T.M., 2008. Ultrastructural studies of oogenesis in the variable abalone *Haliotis varia* (Vetigastropoda : Haliotidae). Aquat. Biol. 2 (2), 143–151. https://doi.org/10.3354/ab00046.

Newman, G.G., 1967. Reproduction of the south African abalone, *Haliotis midae*. Investl. Rep. Div. Sea Fish S Afr. 64, 1–24.

Normand, J., Le Pennec, M., Boudry, P., 2008. Comparative histological study of gametogenesis in diploid and triploid Pacific oysters (*Crassostrea gigas*) reared in an estuarine farming site in France during the 2003 heatwave. Aquaculture 282(1–4), 124–129. doi: https://doi.org/10.1016/j.aquaculture.2008.06.026.

Osterheld, K., Davidson, J., Comeau, L.A., Audet, C., Hori, T., Tremblay, R., 2024. Reproductive investment and gonad development in triploid mussels, *Mytilus Edulis*. Aquaculture 593, 741315. https://doi.org/10.1016/j.aquaculture.2024.741315.

Park, I.S., Gil, H.W., Lee, T.H., Nam, Y.K., Kim, D.S., 2016. Comparative study of growth and gonad maturation in diploid and triploid marine medaka, *Oryzias dancena*. Dev. Reprod. 20 (4), 305–314. https://doi.org/10.12717/dr.2016.20.4.305.

Peruzzi, S., Chatain, B., Saillant, E., Haffray, P., Menu, B., Falguiere, J.C., 2004. Production of meiotic gynogenetic and triploid sea bass, *Dicentrarchus labrax* L. 1. Performances, maturation and carcass quality. Aquaculture 230 (1–4), 41–64. https://doi.org/10.1016/s0044-8486(03)00417-4.

Piferrer, F., Beaumont, A., Falguière, J.C., Flajšhans, M., Haffray, P., Colombo, L., 2009. Polyploid fish and shellfish: production, biology and applications to aquaculture for performance improvement and genetic containment. Aquaculture 293 (3), 125–156. https://doi.org/10.1016/j.aquaculture.2009.04.036.

Przybyl, A., Juchno, D., Przybylski, M., Leska, A., Nowosad, J., Kucharczyk, D., Boron, A., 2022. Sex steroids in diploid and triploid gibel carp (*Carassius gibelio*) of both sexes in different phases of the reproductive cycle. Anim. Reprod. Sci. 244. https://doi.org/10.1016/j.anireprosci.2022.107053.

Qin, Y., Zhang, Y., Yu, Z., 2022. Aquaculture performance comparison of reciprocal triploid *C. gigas* produced by mating tetraploids and diploids in China. Aquaculture 552. https://doi.org/10.1016/j.aquaculture.2022.738044.

Roux, A., Lambrechts, H., Roodt-Wilding, R., 2013. Reproductive histology of cultured *Haliotis midae* (Linnaeus, 1758) and preliminary evaluation of maturation. J. Shellfish Res. 32 (1), 143–153. https://doi.org/10.2983/035.032.0120.

Sakai, T., Yamamoto, T., Matsubara, S., Kawada, T., Satake, H., 2020. Invertebrate gonadotropin-releasing hormone receptor signaling and its relevant biological actions. Int. J. Mol. Sci. 21 (22), 8544. https://doi.org/10.3390/ijms21228544.

Singhakaew, S., Seehabutr, V., Kruatrachue, M., Sretarugsa, P., Romratanapun, S., 2003. Ultrastructure of male germ cells in the testes of abalone, *Haliotis ovina* Gmelin. Molluscan Res. 23 (2), 109–121. https://doi.org/10.1071/mr02016.

Sobhon, P., Apisawetakan, S., Linthong, V., Pankao, V., Wanichanon, C., Meepool, A., Kruatrachue, M., Upatham, E.S., Pumthong, T., 2001. Ultrastructure of the differentiating male germ cells in *Haliotis asinina* Linnaeus. Invertebr. Reprod. Dev. 39 (1), 55–66. https://doi.org/10.1080/07924259.2001.9652467.

Suquet, M., Malo, F., Quere, C., Ledu, C., Le Grand, J., Benabdelmouna, A., 2016. Gamete quality in triploid Pacific oyster (*Crassostrea gigas*). Aquaculture 451, 11–15. https://doi.org/10.1016/j.aquaculture.2015.08.032.

Tiwary B.K., Kirubagaran R., Ray A.K., 2002. Gonadotropin releasing hormone (GnRH) neurones of triploid catfish, *Heteropneustes fossilis* (Bloch): an immunocytochemical study. Comp. Biochem. Physiol. Part A Mol. Integr. Physiol. 132(2), 375–380. doi: https://doi.org/10.1016/S1095-6433(02)00037-5.

Wang, Y., Gan, Y., Zhang, J., Xiao, Q., Shen, Y., Chen, Y., You, W., Luo, X., Ke, C., 2022. Performance of triploid *Haliotis discus hannai* cultured in a subtropical area using sea-based suspended systems. Aquaculture 548. https://doi.org/10.1016/j.aquaculture.2021.737722.

Wu, Q., Song, Z., Wang, L., Wu, Z., Zou, C., Shu, C., Liang, S., Wang, W., Sun, Y., Yue, X., 2023. Comparative study on the gonadal development in the diploid and artificially induced triploid olive flounder *Paralichthys olivaceus*. Aquaculture 565, 739106. https://doi.org/10.1016/j.aquaculture.2022.739106.

Xu, G., Huang, T., Jin, X., Cui, C., Li, D., Sun, C., Han, Y., Mu, Z., 2016. Morphology, sex steroid level and gene expression analysis in gonadal sex reversal of triploid female (XXX) rainbow trout (*Oncorhynchus mykiss*). Fish Physiol. Biochem. 42 (1), 193–202. https://doi.org/10.1007/s10695-015-0129-7.

Yan, S., Li, X., Zhang, G., 2005. Ultrastructure of diploid and triploid abalones, *Haliotis discus hannai* during spermatogenesis. J. Fish. China 03, 289–295.

Yang, H., Guo, X., Scarpa, J., 2019. Tetraploid induction and establishment of breeding stocks for all-triploid seed production. EDIS. FA215. https://doi.org/10.32473/edis-fa215-2019.

Yang, Q., Yu, H., Li, Q., 2022a. Disruption of cell division prevents gametogenesis in triploid Pacific oysters (*Crassostrea gigas*). Aquaculture 560. https://doi.org/10.1016/j.aquaculture.2022.738477.

Yang, Q., Yu, H., Li, Q., 2022b. Refinement of a classification system for gonad development in the triploid oyster *Crassostrea gigas*. Aquaculture 549, 737814. https://doi.org/10.1016/j.aquaculture.2021.737814.

Yang, Q., Yu, H., Du, S., Li, Q., 2024. Overexpression of CDC42 causes accumulation of DNA damage leading to failure of oogenesis in triploid Pacific oyster *Crassostrea gigas*. Int. J. Biol. Macromol. 282, 136769. https://doi.org/10.1016/j.ijbiomac.2024.136769.

Zajicek, P., Goodwin, A.E., Weier, T., 2011. Triploid grass carp: triploid induction, sterility, reversion, and certification. N. Am. J. Fish Manag. 31 (4), 614–618. https://doi.org/10.1080/02755947.2011.608616.